Journal of Pharmaceutical Sciences 109 (2020) 515-523

Contents lists available at ScienceDirect

Journal of Pharmaceutical Sciences

journal homepage: www.jpharmsci.org

Pharmaceutical Biotechnology

Assessment of the Injection Performance of a Tapered Needle for Use in Prefilled Biopharmaceutical Products

Elena Krayukhina [1], Ayano Fukuhara [1], Susumu Uchiyama [1, 2, 3, *]

[1] Research Department, U-Medico Inc., 2-1 Yamadaoka, Suita, Osaka 565-0871, Japan
[2] Department of Biotechnology, Graduate School of Engineering, Osaka University, 2-1 Yamadaoka, Suita, Osaka 565-0871, Japan
[3] Department of Creative Research, Exploratory Research Center on Life and Living Systems (ExCELLS), National Institutes of Natural Sciences, 5-1 Higashiyama, Myodaiji, Okazaki, Aichi 444-8787, Japan

ARTICLE INFO

Article history:
Received 26 July 2019
Revised 17 October 2019
Accepted 17 October 2019
Available online 22 October 2019

Keywords:
injectable(s)
injector(s)
viscosity
high concentration
rheology

ABSTRACT

The design of injection devices, including prefilled syringes (PFSs) and autoinjectors, requires an understanding of the optimization of injection conditions. The injection of highly concentrated biopharmaceuticals can lead to exceptionally high injection forces, due to their high viscosity. To overcome this challenge, a tapered needle has been recently developed by Terumo Corporation. In the present study, we measured the injection forces in PFSs equipped with 24G-29G tapered needle (29G TNN), 27G thin-wall needle (27G TW), and 29G TW using several model and pharmaceutical protein solutions. The injection forces measured in the 29G TNN PFSs were lower than those in 29G TW for all solutions, similar to those in 27G TW PFSs for Newtonian solutions, and were lower than those in the 27G TW PFSs for non-Newtonian solutions which demonstrated shear-thinning behavior. No significant changes in aggregates or micron-size particle concentrations were observed upon injection, regardless of the needle type. Mathematical modeling supported the experimental findings that under similar flow rate conditions injection pressure in a tapered needle is lower than that in a cylindrical needle. Our results indicate that there are advantages of using tapered needles for the injection of biopharmaceutical formulations particularly those showing shear-thinning behavior.

Introduction

Prefilled syringes (PFSs) are increasingly becoming a primary container of choice for parenteral biopharmaceutical products.[1,2] In addition to providing accurate administration of required doses, and being convenient and safe to handle compared to conventional vial packaging,[3] recently developed cyclo-olefin polymer silicone oil-free syringes provide enhanced stability against aggregation,[4,5] and mitigate potential immunogenicity of the biopharmaceuticals.[6] PFSs are an increasingly attractive option for ready-to-use autoinjectable drugs, which are often composed of highly concentrated solutions of biopharmaceutical products. An acceptable level of dynamic injection pressure must be assured for the successful injection of such solutions.[7] In clinical practice, injection pressure is commonly estimated by the injection force, which is a measure of effort required by the user during depression of the plunger on a delivery device. Previous studies have suggested that low exerted injection force was consistent with improved patient convenience and ease of injection.[8-11] The upper limit for the injection force is not specified by the International Organization for Standardization, but in general, it should not exceed a finger push strength that can be comfortably exerted by the users. In accordance with the findings of Peebles and Norris,[12] the lowest value of the mean downwards pushing force of the thumb finger, exerted for 5 s and measured in different segmented age groups ranging from 2 to 90 years old, was 26.9 ± 18.8 N.

The dynamic injection pressure is affected by PFS size, injection speed, and, in particular, needle dimensions.[13-16] Regardless of the PFS used, to decrease injection force, and consequently reduce injection pain and patient anxiety, careful consideration should be given to the needle diameter and design.[17] Extra-thin wall pen needles with diameters of 31G and 32G used for injection of insulin provided statistically better performance compared to usual pen needles and were associated with lower thumb force required to

This article contains supplementary material available from the authors by request or via the Internet at https://doi.org/10.1016/j.xphs.2019.10.033.

* *Correspondence to:* Susumu Uchiyama (Telephone: +81-6-6879-7441).
E-mail address: suchi@bio.eng.osaka-u.ac.jp (S. Uchiyama).

https://doi.org/10.1016/j.xphs.2019.10.033
0022-3549/

inject a full dose.[9] Unfortunately, thin needles, with diameters smaller than 30G, which cause minimal pain, are generally not suitable for the injection of highly concentrated drug formulations.[18] To reduce viscous resistance to flow through the needle, needles with either a larger diameter or a shorter length can be used. Another approach is to employ a tapered needle, which has a larger diameter at its proximal end than at a distal end. When used with non-Newtonian fluids, the increase in shear force provided by taper may decrease the resistance to flow, leading to a decrease in injection pressure.

Numerous theoretical studies have been conducted in order to describe the flow of Newtonian and non-Newtonian fluids in tapered tubes,[19-23] whereas experimental studies to confirm derived theoretical predictions are rather limited. Nevertheless, the injection performance benefits of tapered needles have been clearly demonstrated. Similar flow characteristics were revealed for a tapered 22G-27G spinal needle (Temena-Polymedic) and a conventional 22G spinal needle (Becton-Dickinson), whereas tapered needle was potentially associated with a lower incidence of post-dural puncture headaches.[24] A clinical study conducted to evaluate injection performance of different needles upon self-injection of insulin revealed that even though the injection forces in 28G-33G microtapered needles (Terumo Corporation, Tokyo, Japan) were similar to those in standard 31G thin-wall (TW) needles (Becton-Dickinson), patients concerned about pain often preferred microtapered needle over TW needle.[25] These results suggest a potential role of tapering technology in reducing pain and discomfort of injections when compared with traditional needles. Based on these findings, to enable efficient injection of highly viscous drug products while minimizing injection forces and associated pain, Terumo Corporation recently developed the 24G-29G tapered needle (29G TNN), which combines the effects of diameter and length (Fig. 1).

In the study reported here, we performed functional evaluation of PFSs equipped with 27G TW, 29G TW, or 29G TNN needles for injection of highly viscous formulations of biotherapeutic products using glycerin, polyethylene glycol (PEG 3350), carboxymethyl cellulose sodium salt (CMC), and solutions of 2 pharmaceutical proteins. Injectability tests showed that the injection forces in 29G TNN PFSs were lower than those in 29G TW PFSs for all solutions, and were similar to those in 27G TW PFSs, with the exception of the CMC and a highly concentrated protein solution, for which the injection forces in 29G TNN PFSs were actually lower than those in 27G TW PFSs. Measurements of shear viscosity confirmed the shear-thinning behavior of these solutions. According to previously described mathematical models of shear rate,[26,27] we estimated that for the shear-thinning solutions, the injection force in 29G TNN PFS is equivalent to injection using a cylindrical needle of the same length with a diameter larger than 25G. Mathematical modeling supported the experimental results, demonstrating that under the same flow rate conditions, the injection pressure in a tapered needle is lower than that in a cylindrical needle. Distribution profiles of aggregates and micron-size particles were similar among PFSs with different needles, and it was confirmed that needle clogging does not occur during quiescent storage for up to 3 weeks at 5°C or 25°C. When injection was performed into porcine tissue as a model of human subcutaneous tissue, a similar increase of ~1.2-fold in injection force was observed in all PFSs. These results suggest that a tapered needle can provide superior performance compared to a cylindrical needle, particularly for use with highly concentrated prefilled biopharmaceutical products.

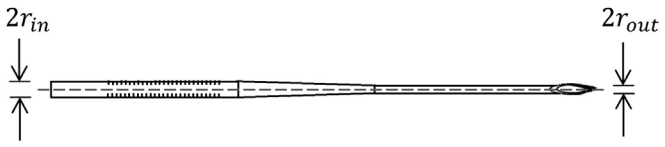

Figure 1. Schematic representation of the 29G TNN.

Materials and Methods

Materials and Sample Preparations

Syringes

Silicone oil-free PLAJEX™ 1-mL long cyclo-olefin polymer PFSs with chlorinated butyl rubber plunger stoppers coated using a proprietary i-coating™ technique,[28] equipped with either a 27G TW, a 29G TW needle, a 29G TNN, or a luer lock, were obtained from Terumo Corporation.

Model Solutions

Glycerin, 50% w/v PEG 3350, and CMC were purchased from Nacalai Tesque, Inc. (Tokyo, Japan). Glycerin solutions at concentrations of 60%, 70%, 75%, and 80% w/w, PEG 3350 solutions at concentrations of 20%, 30%, 40%, and 48% w/v, and CMC solutions at concentrations of 0.5%, 1.0%, 1.25%, and 1.5% w/w were prepared using Milli-Q water. Approximately 0.5 mL of each solution was placed into 27G TW, 29G TW, and 29G TNN PFSs, and the PFSs were sealed with plunger stoppers, leaving no headspace. Three PFSs of each type were used. PFSs were kept at room temperature overnight before being used for injection force measurements.

Therapeutic Proteins

Etanercept (Enbrel), a dimeric fusion protein consisting of the extracellular ligand-binding portion of the human 75 kDa (p75) tumor necrosis factor receptor linked to the Fc portion of IgG1, was purchased as a lyophilized powder (25 mg/vial) for intravenous infusion (Amgen Inc., Thousand Oaks, CA). One milliliter of water for injections (WFI) (Otsuka Pharmaceutical Company, Ltd., Tokyo, Japan) was added to obtain reconstituted solution of etanercept at a concentration of 25 mg/mL, and etanercept at a concentration of 1 mg/mL was obtained by dilution of the 25 mg/mL solution using formulation buffer. Omalizumab (Xolair), a recombinant DNA-derived humanized IgG1κ monoclonal antibody that selectively binds to human immunoglobulin E, was purchased as a lyophilized powder (150 mg/vial) for subcutaneous injections (Novartis Pharma K.K., Tokyo, Japan). Either 1.4 mL or 2.5 mL of WFI was added to obtain reconstituted solutions of omalizumab at concentrations of 125 and 70 mg/mL, respectively. Approximately 0.5 mL of each protein solution was placed into 27G TW, 29G TW, 29G TNN, and luer lock PFSs, and the PFSs were sealed with plunger stoppers, leaving no headspace. To test the impact of injection volume on injection force, measurements using 1 mL of 125 mg/mL omalizumab solution were performed. Three PFSs of each type were used. PFSs were kept at 25°C overnight before being used for injection force measurements.

Methods

Injection Force Measurements

Injection forces were measured using a texture analyzer EZ-SX with a 100 N force sensor (Shimadzu Corporation, Kyoto, Japan) at room temperature. Syringes were emptied by pushing down the plunger at a constant injection speed with a stroke distance of 13 mm and 26 mm using PFSs filled with 0.5 and 1 mL of sample, respectively. The needle tips were left open to the atmosphere, and dispensed samples were collected using a microcentrifuge tube. Glycerin, PEG 3350, and CMC were measured using 27G TW, 29G TW, and 29G TNN PFSs at injection speeds of 3 mL/min and 6 mL/min. Protein solutions were measured using 27G TW, 29G TW, 29G TNN, and luer lock PFSs at an injection speed of 6 mL/min. Injection forces

are reported as the highest force measured before the plunger reached the predefined stroke distance.

The possible needle clogging during storage was assessed by measuring injection forces in PFSs filled with 125 mg/mL omalizumab solution after overnight incubation at 25°C, storage at 5°C or 25°C for 1 and 3 weeks and comparing the resulting values. A 29G TW PFS was exposed to heating at 60°C for 5 min using a heated air stream as a positive control.

In order to assess injection forces as close as possible to *in vivo* conditions, the injection forces were measured *ex vivo* using porcine tissue as a suitable model for human subcutaneous injections.[29] Fresh abdominal subcutaneous and muscle tissue specimen from 6-month-old castrated landrace male pig cut into cubes of 4 cm × 6 cm with thickness larger than 3 cm was purchased from Domestic Animal Resource Development Company, Ltd. (Tokyo, Japan). Prior to measurement, tissues were incubated in a water bath at 30°C for 1 h. The 27G TW, 29G TW, and 29G TNN PFS needle was manually inserted ~0.8 cm underneath the skin, and injection force was measured at an injection speed of 6 mL/min. Control measurements into air were performed prior to injection into subcutaneous tissue to exclude possible differences in injection forces caused by lot-to-lot sample variability.

Viscosity Measurements

The kinematic viscosities were measured at 20°C using a rolling-ball viscometer Lovis 2000 M/ME (Anton Paar, Graz, Austria) and converted to dynamic viscosities using the respective densities, measured using a density meter DMA 5000 (Anton Paar) at 20°C. Shear rate-dependent viscosities of glycerin (60% and 80%), CMC (0.50% and 1.50%), and omalizumab (70 and 125 mg/mL) solutions were measured using an MCR 302 rotational rheometer (Anton Paar) equipped with a cone-plate sensor with a diameter of 35 mm, a cone angle of 1°, and a gap of 0.066 mm. For the etanercept (1 and 25 mg/mL) measurements, a cone-plate sensor with a diameter of 50 mm, a cone angle of 1°, and a gap of 0.108 mm was used. Shear rates of up to 15,000 s^{-1} were applied, and the plate temperature was maintained at 23°C using a Peltier temperature-controlled system. Tests were started 180 s after closing the measuring gap.

Size Exclusion Chromatography

Size exclusion chromatography measurements were performed using an Alliance HPLC system (Waters, Milford, MA) equipped with a TSKgel G3000SWXL column (Tosoh Bioscience, Tokyo, Japan) with simultaneous UV absorbance detection at 215 and 280 nm using 1× phosphate buffered saline (pH 7.4) (Thermo Fisher Scientific K.K., Tokyo, Japan) as the mobile phase. After dilution of etanercept and omalizumab samples to a concentration of 1 mg/mL, 20 μL aliquots were injected into the HPLC system. The flow rate was set at 0.5 mL/min and the elution time at 30 min.

Flow Imaging Analysis

Flow imaging measurements of etanercept and omalizumab samples were performed using a FlowCam 8100 system (Fluid Imaging Technologies, Inc., Scarborough, ME). Sufficient amount of Milli-Q water was used to obtain a particle-free baseline. Sample volumes of 0.15 mL were analyzed at a flow rate of 0.05 mL/min using Fluid Imaging Technologies VisualSpreadsheet version 4.1.95 (Fluid Imaging Technologies, Inc.).

Results

Injection Forces for Glycerin, PEG 3350, and CMC Solutions

For glycerin solutions at concentrations 0%–80% w/w, the injection forces were linearly proportional to the viscosities. The injection force in 29G TNN PFS was lower than that in 29G TW PFS, and similar to that in 27G TW PFS at both injection speeds (Figs. 2a and 2b). This result indicates that 29G TNN reduces the injection force in PFS compared with 29G TW.

Injection force F can be described using Hagen–Poiseuille's equation[26]

$$F = F_{friction} + \frac{8QlR^2}{r^4}\eta \quad (1)$$

where $F_{friction}$ corresponds to frictional force between syringe barrel and stopper, Q to volumetric flow rate (m^3/s), l to length of needle (m), R to inner syringe radius (m), r to inner needle radius (m), and η to dynamic viscosity (Pa·s). Using the above equation, we fitted the measured values of injection forces and determined frictional forces from the intercept of the resulting curve (Supplementary Information Table S1). We also calculated the apparent needle radii from the slope. For 29G TNN, we neglected the taper and assumed a uniform radius throughout its length. The resulting values for 27G TW and 29G TW (Table 2) were in a good agreement with the specification values (Table 1). The apparent radius for 29G TNN was similar to that of 27G TW at both injection speeds (Table 2).

As with glycerin solutions, PEG 3350 solutions at concentrations 0%–48% v/w exhibited injection forces in 29G TNN PFS similar to those in 27G TW PFS, and lower than those of 29G TW PFS at both injection speeds (Supplementary Information Fig. S1). As with glycerin, we evaluated apparent needle radii using Equation 1 and found that for 27G TW and 29G TW the resulting values (Table 2) were in a good agreement with the specification values (Table 1). For 29G TNN, the apparent radius was similar to that of 27G TW at both injection speeds, a finding which explains the similarities between the injection forces measured for 29G TNN PFS and 27G TW PFS.

In the case of CMC solutions at concentrations 0%–1.5%, the injection forces measured in all PFSs were non-linearly proportional to the viscosity of their contents, and were actually lower than the values calculated using Equation 1 (Figs. 2c and 2d). We hypothesize that this observation is due to a shear-thinning phenomenon occurring at high shear rates, as has been previously reported for CMC solutions.[30] In contrast to the results obtained for glycerin and PEG 3350 solutions, for CMC solutions at both injecting speeds, the injection force in 29G TNN PFS was lower than that in both 29G TW PFS and 27G TW PFS. These results suggest that 29G TNN is capable of producing a lower injection force compared with 29G TW and 27G TW upon the injection of shear-thinning non-Newtonian fluids.

Injection Forces for Protein Solutions

Similar low values for injection force were obtained for etanercept solutions at concentrations of 1 and 25 mg/mL, regardless of the needle type (Fig. 3a). At 1 mg/mL, there were no significant differences among the values for PFSs with different needles, whereas at 25 mL/min, the injection force for 29G TNN PFS appeared to be slightly higher than those of the other PFSs. This finding is consistent with the result obtained for WFI, where the injection force was of a few Newtons and appeared to be somewhat higher in 29G TNN PFS than in 27G TW PFS and 29G TW PFS. This discrepancy is due to slightly higher frictional forces in the 29G TNN PFS compared with 27G TW PFS and 29G TW PFS, which make the major contribution to injection force of solutions with relatively low viscosities, such as those of etanercept at a concentration of 1 mg/mL (1.0 cP) and 25 mg/mL (2.2 cP).

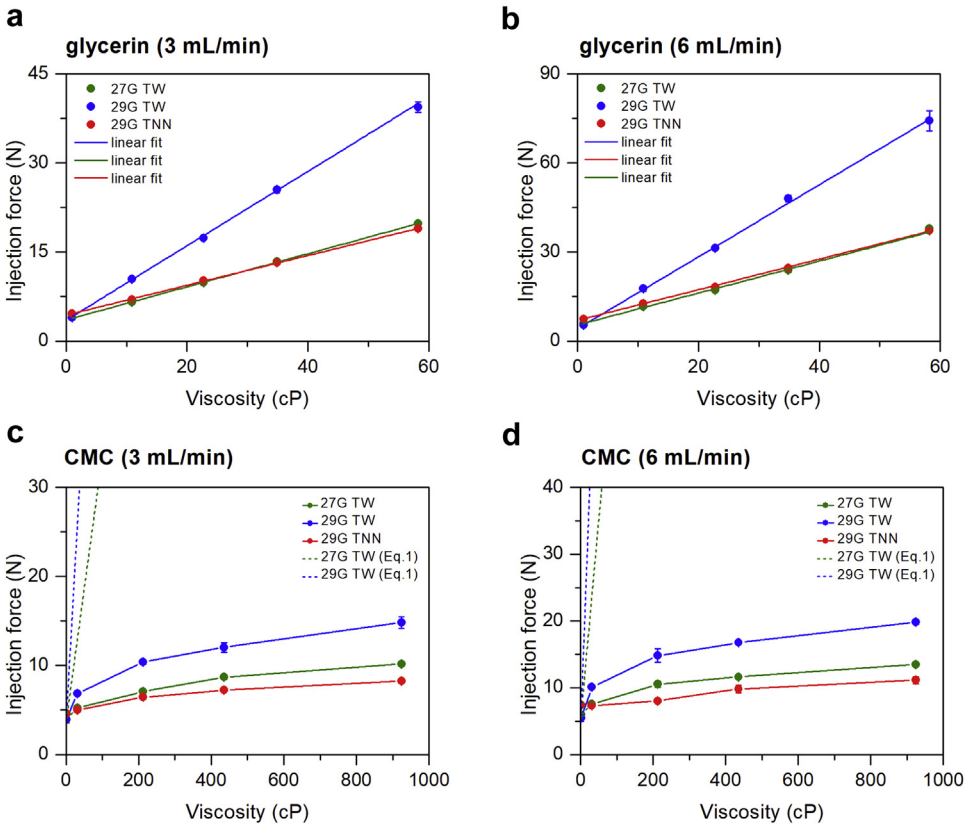

Figure 2. Injection forces measured at injection speeds of 3 and 6 mL/min in 27G TW (green circles), 29G TW (blue circles), and 29G TNN (red circles) PFSs and plotted as a function of the dynamic viscosity: (a) glycerin at 3 mL/min, (b) glycerin at 6 mL/min, (c) CMC at 3 mL/min, and (d) CMC at 6 mL/min. The solid lines in (a and b) represent the linear fits. The solid lines in (c and d) connecting data points are added as visual guides. The dashed lines in (c and d) represent injection forces calculated using Equation 1. Data represent the mean of triplicate measurements, with error bars corresponding to the standard error of the mean.

In contrast to etanercept, omalizumab solutions at concentrations of 70 and 125 mg/mL had relatively high dynamic viscosity values of 11 and 104 cP, respectively. For 70 mg/mL omalizumab, the injection force for 29G TNN PFS was similar to that in 27G TW PFS and was lower than that of 29G TW PFS (Fig. 3b). For the 125 mg/mL solution, the lowest injection force was measured for 29G TNN PFS, followed by 27G TW PFS and 29G TW PFS. The acquired graph profiles were similar in shape for all PFSs with no extra peaks at the beginning of the injection, whereas the injection force plateau height was lowest for 29G TNN PFS (Fig. 3c). These results suggest the absence of a high plunger-stopper break loose force and indicate that 29G TNN was capable of reducing the injection force for 125 mg/mL omalizumab.

To assess the possible effect of injection volume on injection force, in addition to 0.5 mL, we performed measurements using 1 mL of 125 mg/mL omalizumab solution. Regardless of the injected volume, the obtained curves were similar in shape. During the beginning of injection, the injection force increased at the same rate for both injection volumes and reached plateaus of the same amplitude, but of different durations (Fig. S2). The plateau in the curve corresponding to the 1-mL injection was prolonged compared to that of the 0.5-mL injection due to the extended injection duration. This result suggests that under similar injection conditions, the resulting injection force is independent of the injection volume.

Stability of Protein Solutions Upon Injection

To evaluate the effect of needle geometry, size, and the resulting shear stress on the stability of pharmaceutical proteins during injection, soluble aggregates and larger insoluble particles were characterized in the pharmaceutical protein solutions after injection force experiments using size exclusion chromatography and flow imaging analysis, respectively. No considerable changes in aggregate concentrations were observed in all solutions regardless of the needle type used (Figs. 4a and 4c), in agreement with the previously published finding that shear rates up to 250,000 s^{-1} do not cause considerable protein aggregation.[31] Similarly, low levels of micron-size particles were present in all samples regardless of the needle type (Figs. 4b and 4d). These results suggest that protein stability is not affected by any of the needles used in the present study.

Table 1
Dimensions of PFSs Used in the Present Study

Parameter	29G TW PFS	27G TW PFS	29G TNN PFS
Syringe inner radius (R) (mm)	3.150 ± 0.025	3.150 ± 0.025	3.150 ± 0.025
Length of the needle (l) (mm)	21.9 ± 0.5	21.9 ± 0.5	22.0 ± 0.4
Needle inner radius (r) (mm)	0.105 ± 0.010	0.131 ± 0.010	0.233 (r_{in}) 0.119 (r_{out})

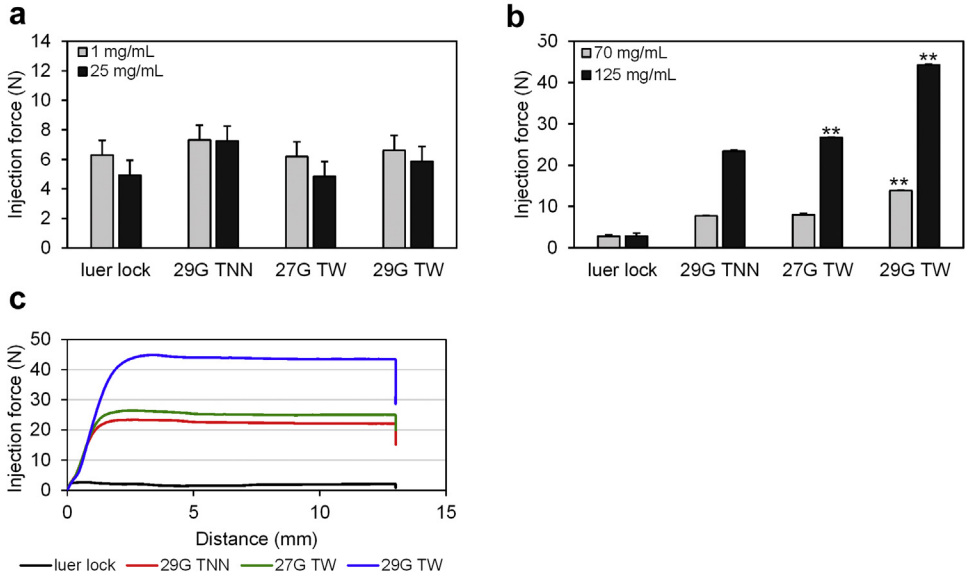

Figure 3. Injection forces measured at an injection speed of 6 mL/min in 29G TNN, 27G TW, 29G TW, and luer lock PFSs: (a) etanercept at a concentration of 1 mg/mL (gray) and 25 mg/mL (black) and (b) omalizumab at a concentration of 70 mg/mL (gray) and 125 mg/mL (black). Data represent the mean of triplicate measurements, with error bars corresponding to the standard error of the mean. $^{**}p < 0.01$ (2-sample t-test assuming equal variances). Representative force-displacement profiles for 125 mg/mL omalizumab in 29G TNN (red), 27G TW (green), 29G TW (blue), and luer lock (black) PFSs are shown in (c).

Needle Clogging Assessment

Possible needle clogging during storage is of concern for highly concentrated biopharmaceutical products formulated in PFSs with a staked-in needle.[32] To evaluate the effect of needle geometry in combination with different storage conditions on extent of clog formation, we measured injection forces in 27G TW, 29G TW, and 29G TNN PFSs filled with 125 mg/mL omalizumab solution after overnight incubation at 25°C, storage at 5°C or 25°C for 1 and 3 weeks, and compared the resulting profiles. Regardless of the storage temperature and period, the force-displacement curves were similar for the same PFS type, with the injection force steadily reaching plateau after an initial plunger displacement of ~2 mm (Fig. S3). In contrast, in a clogged control sample, the injection force first increased to its maximum value that was ~2-fold higher than that in the normal sample, and then, within plunger displacement of ~3 mm, reached a plateau value similar to that of a non-clogged sample, which is consistent with the force profile of a partially clogged needle.[33] This result suggests that 27G TW, 29G TW, and 29G TNN clogging does not occur during quiescent PFS storage for up to 3 weeks at 5°C or 25°C. However, further studies are required to assess the potential needle clogging during extended storage periods.

Effect of Subcutaneous Tissue on the Injection Force

The target tissues may provide a high resistance to injection flow, generating additional increase in injection pressure. Therefore, to ensure acceptable levels of injection pressure in systems designed to deliver highly concentrated biopharmaceuticals, in addition to designing optimization during development, it is desirable to investigate the tissue compliance during usability testing.[34]

To assess the resistance of subcutaneous tissue during injection, the force required to inject 125 mg/mL omalizumab solution was measured using porcine tissue as a suitable model for human subcutaneous injections.[29] The resulting force-displacement curves were similar in shape, and the injection forces upon injection into subcutaneous tissue were ~1.2-fold higher compared to the injection into air due to additional tissue resistance (Fig. S4). This result

Table 2
Apparent Needle Radii (mm) Calculated From Injection Force Measurements

Solution	Shear Rate	29G TW		27G TW		29G TNN	
		Injection Speed (mL/min)					
		3	6	3	6	3	6
Glycerin[a]	NA	0.109	0.110	0.133	0.133	0.136	0.135
PEG 3350[a]	NA	0.107	0.108	0.132	0.132	0.134	0.133
CMC (0.5%)	γ_w[b]	0.107	0.104	0.137	0.142	0.191	0.238
	γ_{eff}[c]	0.109	0.107	0.141	0.145	0.195	0.244
CMC (1.5%)	γ_w	0.089	0.089	0.113	0.116	0.143	0.155
	γ_{eff}	0.103	0.103	0.131	0.135	0.166	0.179
Omalizumab (125 mg/mL)	γ_w	NA	0.115	NA	0.140	NA	0.152
	γ_{eff}	NA	0.115	NA	0.141	NA	0.153

NA, not applicable.
[a] Measured injection force values are plotted as a function of the measured viscosity, then linear regression analysis using Equation 1 was performed, and the apparent needle radius was determined from the slope of the resulting curve.
[b] The expression for the wall shear rate γ_w is given by Equation 3.
[c] The expression for the "effective" shear rate γ_{eff} is given by Equation 4.

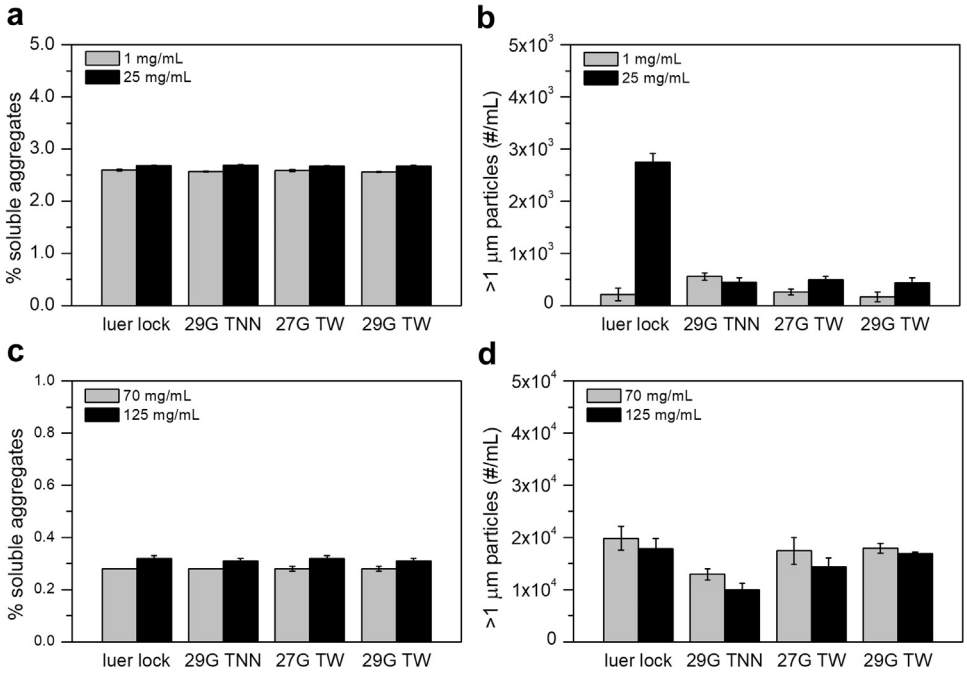

Figure 4. Effect of needle geometry on stability of pharmaceutical proteins. Concentrations of aggregates and micron-size particles in etanercept at concentrations of 1 mg/mL (gray) and 25 mg/mL (black) (a and b) and omalizumab at concentrations of 70 mg/mL (gray) and 125 mg/mL (black) (c and d) were measured after injection using 29G TNN, 27G TW, 29G TW, and luer lock PFSs. Data represent the mean of triplicate measurements, with error bars corresponding to the standard error of the mean.

is consistent with previously published studies, where injection was performed into the abdominal skin obtained from a Eurasian female donor who underwent cosmetic surgery.[7]

Discussion

To explain why 29G TNN was capable of reducing injection forces compared with 27G TW for some solutions, while not for others, and to test our hypothesis that 29G TNN can be particularly effective in reducing injection forces for solutions exhibiting shear-thinning behavior, we measured the viscosity of glycerin, CMC, and protein solutions as a function of shear rate. Even though in 27G TW and 29G TW, at an injection speed of 6 mL/min shear rates of ~57,000 and 84,000 s^{-1} can be achieved, for the measurements using a cone-plate rheometer, technically feasible shear rates of up to 15,000 s^{-1} were applied. As expected, the viscosity of the glycerin solutions was independent of shear rate (Figs. 5a and 5b), whereas the viscosity of the CMC solutions decreased with increasing shear rate, and the magnitude of the decrease was larger for the solutions of higher concentration (Figs. 5c and 5d). The viscosity of etanercept at 1 and 25 mg/mL was only a few centipoises, and did not exhibit an explicit shear rate dependence (Figs. 5e and 5f). Likewise, the viscosity of omalizumab at a concentration of 70 mg/mL appeared to be shear rate independent (Fig. 5g). In contrast, the viscosity profile of omalizumab at a concentration of 125 mg/mL showed a shear-independent region up to 3000 s^{-1}, followed by a rapid decrease with increasing shear rates (Fig. 5h). In this region, the dynamic viscosity η can be expressed in terms of shear rate γ, using the Ostwald–de Waele equation

$$\eta = K\gamma^{n-1} \tag{2}$$

where K is a consistency index and n is a power law index. We plotted the logarithm of the dynamic viscosity versus the logarithm of the shear rate, and used linear regression analysis to determine the slope and intercept, which correspond to $n-1$ and K, respectively (Supplementary Information Table S2). The resulting power law index values for the CMC and 125 mg/mL omalizumab solutions were less than 1, further confirming their characteristic shear-thinning behavior.

From the injection forces measured for CMC and omalizumab, we calculated the apparent needle radii. We substituted the expression for η from Equation 2 into 1. Shear rate dependence on n was defined using 2 different approaches that have been previously reported. Rathore et al.[27] showed that the maximum shear rate γ_w at the wall may be expressed as

$$\gamma_w = \left(\frac{3n+1}{n}\right)\frac{Q}{\pi r^3} \tag{3}$$

An expression for the "effective" shear rate γ_{eff} that takes into consideration non-linear shear rate changes throughout the needle diameter was proposed by Allmendinger et al.[26]

$$\gamma_{eff} = \left(\frac{3n+1}{2n+1}\right)\frac{2Q}{\pi r^3} \tag{4}$$

Substituting the expression for γ from Equations 3 and 4 into Equation 1 gives the following equations, which describe the injection force of a non-Newtonian fluid in a syringe equipped with a cylindrical needle:

$$F = F_{friction} + 8\pi^{1-n} lR^2 KQ^n r^{-(3n+1)}\left(\frac{3n+1}{n}\right)^{n-1} \tag{5}$$

$$F = F_{friction} + 2^{n+2}\pi^{1-n} lR^2 KQ^n r^{-(3n+1)}\left(\frac{3n+1}{2n+1}\right)^{n-1} \tag{6}$$

Using Equations 5 and 6, we calculated the apparent radii, assuming a uniform radius throughout the length of the needles.

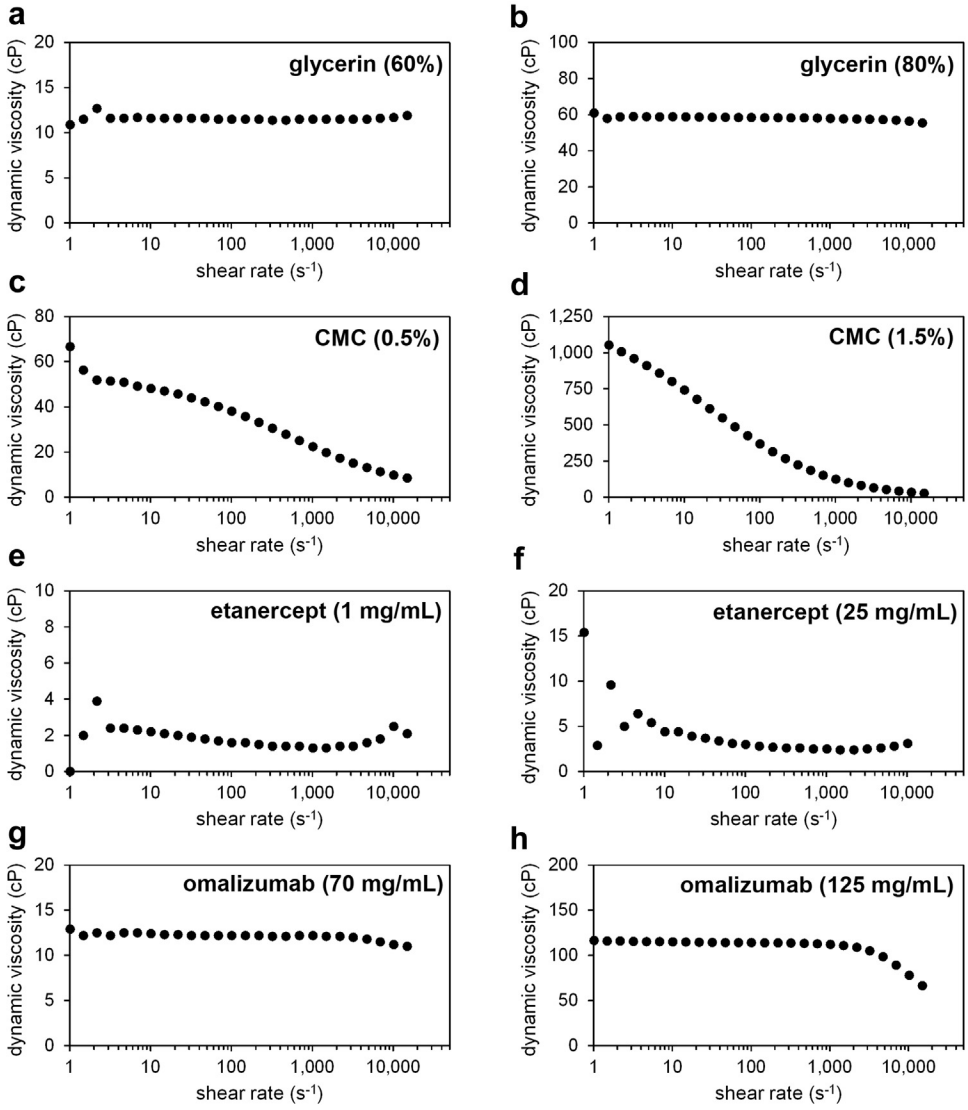

Figure 5. Profiles of viscosities of glycerin at concentrations of 60% (a) and 80% (b), CMC at concentrations of 0.50% (c) and 1.50% (d), etanercept at concentrations of 1 mg/mL (e) and 25 mg/mL (f), omalizumab at concentrations of 70 mg/mL (g) and 125 mg/mL (h).

The resulting values for 27G TW and 29G TW were in good agreement with those obtained from the glycerin and PEG 3350 measurements, whereas for 29G TNN, the calculated apparent radii were considerably larger (Table 2). Thus, when the injectable solution has a shear-thinning property, for a given flow rate, injection using 29G TNN is equivalent to injection using a cylindrical needle of the same length with a diameter larger than 25G.

To further explain the correlation between the non-Newtonian shear-thinning behavior and the reduction in the injection force for tapered needles, we attempted to mathematically describe the effect of needle geometry on a flow rate. The flow rate of Newtonian solution in cylindrical needle Q_c is defined by Hagen–Poiseuille's law:

$$Q_c = \frac{\pi \Delta p r^4}{8\eta l} \tag{7}$$

In a slightly tapered needle, a flow rate can be described using modified Hagen–Poiseuille's equation with so-called lubrication approximation, in which the flow between non-parallel surfaces is treated locally as a flow between parallel surfaces:

$$Q_t = \frac{\pi \Delta p r_{out}^4}{8\eta l}\left[\frac{3(\lambda-1)}{1-\lambda^{-3}}\right] \tag{8}$$

where $\lambda = r_{in}/r_{out}$ is a taper ratio. For 29G TNN, r_{in} is 24G and r_{out} is 29G, and therefore $\lambda > 1$. Under identical conditions, the same flow rate as in the tapered needle can be achieved in the cylindrical needle with an effective radius r_{eff}

$$r_{eff} = \left[r_{out}\frac{3(\lambda-1)}{1-\lambda^{-3}}\right]^{\frac{1}{4}} \tag{9}$$

For a non-Newtonian solution, which can be described with a power law equation, the flow through a cylindrical needle can be expressed as

$$Q_c = \frac{\pi r^3}{1/n+3}\left[\frac{\Delta p r}{2Kl}\right]^{\frac{1}{n}} \tag{10}$$

whereas the flow through a tapered needle is given by[19]

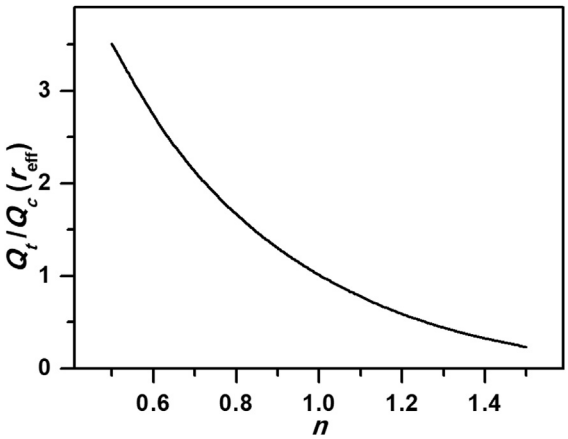

Figure 6. Ratio of the flow in a tapered needle Q_t to the flow in a cylindrical needle with the effective radius $Q_c(r_{eff})$, plotted as a function of the power law index n. For a Newtonian fluid ($n = 1$), flows are equivalent; for shear-thinning fluids ($n < 1$), the flow ratio is greater than 1; and for shear-thinning fluids ($n > 1$), the flow ratio is smaller than 1.

$$Q_t = \frac{\pi r_{out}^3}{1/n+3}\left[\frac{\Delta p r_{out}}{2Kl}\right]^{\frac{1}{n}}\left[\frac{3(\lambda-1)}{1-\lambda^{-3n}}\right]^{\frac{1}{n}} \quad (11)$$

By inserting an expression for r_{eff} into Equation 7 and assuming other conditions to be similar, the ratio of the flow in a tapered needle to that of the flow in a cylindrical needle with the effective radius as a function of the rheological properties of the solution can be described as

$$\frac{Q_t}{Q_c\left(r_{eff}\right)} = \left[\frac{1-\lambda^{-3}}{3(\lambda-1)}\right]^{\frac{3n+1}{4}}\left[\frac{3(\lambda-1)}{1-\lambda^{-3n}}\right]^{\frac{1}{n}} \quad (12)$$

Thus, for a given pressure, the flow rate of shear-thinning solution ($n < 1$) in a tapered needle is higher than that in a cylindrical needle, with the difference being higher for stronger shear-thinning behavior or smaller n-values (Fig. 6). This result suggests that a lower pressure, and consequently lower injection force, can be applied to a tapered needle system to obtain the same flow rate, as compared to a cylindrical needle system. This finding also implies that a tapered needle can provide additional injection benefits for shear-thinning solutions of concentrated biopharmaceuticals.

Conclusions

In the present study, we estimated injection forces in 27G TW, 29G TW, and 29G TNN 1-mL PFSs using glycerin, PEG 3350, CMC, etanercept, and omalizumab solutions. The injection forces in 29G TNN PFSs were lower than those in 29G TW for all solutions, and were similar to those in 27G TW PFSs for glycerin, PEG 3350, etanercept, and 70 mg/mL omalizumab solutions, and were actually lower than those in 27G TW PFSs for CMC and 125 mg/mL omalizumab solutions. The injection forces for 0.5 and 1 mL of 125 mg/mL omalizumab solutions were similar for the same PFS type. Our calculations showed that the reduction in the injection forces in 29G TNN compared to 27G TW was equivalent to injection using a cylindrical needle of the same length with diameter larger than 25G. Shear rate dependent viscosity measurements confirmed the shear-thinning behavior of CMC and 125 mg/mL omalizumab solutions and shear rate independent behavior for the other solutions. Mathematical modeling suggested that under the same pressure conditions, tapered needles produce higher flow rates than cylindrical needles. At equivalent flow rate pressure, and consequently, injection force, in a tapered needle is lower than that in a cylindrical one. No significant changes in aggregates and micron-size particle concentrations upon injection were observed regardless of the needle type. Using 125 mg/mL omalizumab solution, it was confirmed that regardless of the needle type, clogging does not occur during quiescent storage for up to 3 weeks at 5°C or 25°C. When injection was performed into porcine tissue as a model of human subcutaneous tissue, a similar increase of ~1.2-fold in injection force was observed in all PFSs. These results suggest that 29G TNN is capable of providing enhanced injection performance for use in highly concentrated biopharmaceutical products demonstrating shear-thinning behavior.

Acknowledgments

The authors would like to thank Terumo Corporation for providing PFSs and for the helpful discussions.

References

1. Uchiyama S. Liquid formulation for antibody drugs. *Biochim Biophys Acta*. 2014;1844(11):2041-2052.
2. Sacha G, Rogers JA, Miller RL. Pre-filled syringes: a review of the history, manufacturing and challenges. *Pharm Dev Technol*. 2015;20(1):1-11.
3. Makwana S, Basu B, Makasana Y, Dharamsi A. Prefilled syringes: an innovation in parenteral packaging. *Int J Pharm Investig*. 2011;1(4):200-206.
4. Krayukhina E, Tsumoto K, Uchiyama S, Fukui K. Effects of syringe material and silicone oil lubrication on the stability of pharmaceutical proteins. *J Pharm Sci*. 2015;104(2):527-535.
5. Maruno T, Watanabe H, Yoneda S, et al. Sweeping of adsorbed therapeutic protein on prefillable syringes promotes micron aggregate generation. *J Pharm Sci*. 2018;107(6):1521-1529.
6. Krayukhina E, Yokoyama M, Hayashihara KK, et al. An assessment of the ability of submicron- and micron-size silicone oil droplets in dropped prefillable syringes to invoke early- and late-stage immune responses. *J Pharm Sci*. 2019;108(7):2278-2287.
7. Cilurzo F, Selmin F, Minghetti P, et al. Injectability evaluation: an open issue. *AAPS PharmSciTech*. 2011;12(2):604-609.
8. Toraishi K, Yuizono Y, Nakamura N, et al. Force requirements and insulin delivery profiles of four injection devices. *Diabetes Technol Ther*. 2005;7(4):629-635.
9. Aronson R, Gibney MA, Oza K, Berube J, Kassler-Taub K, Hirsch L. Insulin pen needles: effects of extra-thin wall needle technology on preference, confidence, and other patient ratings. *Clin Ther*. 2013;35(7):923-933.e924.
10. van der Burg T. Injection force of SoloSTAR(R) compared with other disposable insulin pen devices at constant volume flow rates. *J Diabetes Sci Technol*. 2011;5(1):150-155.
11. Clarke A, Spollett G. Dose accuracy and injection force dynamics of a novel disposable insulin pen. *Expert Opin Drug Deliv*. 2007;4(2):165-174.
12. Peebles L, Norris B. Filling "gaps" in strength data for design. *Appl Ergon*. 2003;34(1):73-88.
13. Burckbuchler V, Mekhloufi G, Giteau AP, Grossiord JL, Huille S, Agnely F. Rheological and syringeability properties of highly concentrated human polyclonal immunoglobulin solutions. *Eur J Pharm Biopharm*. 2010;76(3):351-356.
14. Rathore N, Pranay P, Eu B, Ji W, Walls E. Variability in syringe components and its impact on functionality of delivery systems. *PDA J Pharm Sci Technol*. 2011;65(5):468-480.
15. Fischer I, Schmidt A, Bryant A, Besheer A. Calculation of injection forces for highly concentrated protein solutions. *Int J Pharm*. 2015;493(1-2):70-74.
16. Adler M. Challenges in the development of pre-filled syringes for biologics from a formulation scientist's point of view. Available at: https://www.americanpharmaceuticalreview.com/Featured-Articles/38372-Challenges-in-the-Development-of-Pre-filled-Syringes-for-Biologics-from-a-Formulation-Scientist-s-Point-of-View/. Accessed September 30, 2019.
17. Iwanaga M, Kamoi K. Patient perceptions of injection pain and anxiety: a comparison of NovoFine 32-gauge tip 6 mm and Micro Fine Plus 31-gauge 5 mm needles. *Diabetes Technol Ther*. 2009;11(2):81-86.
18. Jezek J, Rides M, Derham B, et al. Viscosity of concentrated therapeutic protein compositions. *Adv Drug Deliv Rev*. 2011;63(13):1107-1117.
19. Oka S. Pressure development in a non-Newtonian flow through a tapered tube. *Rheologica Acta*. 1973;12(2):224-227.
20. Oka S. The steady flow of an incompressible Newtonian liquid through a conical nozzle. *Prog Polym Phys Jpn*. 1963;6:71-72.
21. Oka S, Murata T. Theory of the steady slow motion of non-Newtonian fluids through a tapered tube. *Jpn J Appl Phys*. 1969;8(1):5-8.

22. Oka S, Takami A. The steady slow motion of a non-Newtonian liquid through a tapered tube. *Jpn J Appl Phys*. 1967;6(4):423.
23. Nishimura J, Oka S. The steady flow of a viscous fluid through a tapered tube. *J Phys Soc Jpn*. 1965;20:449-453.
24. Ginosar Y, Smith Y, Ben-Hur T, et al. Novel pulsatile cerebrospinal fluid model to assess pressure manometry and fluid sampling through spinal needles of different gauge: support for the use of a 22 G spinal needle with a tapered 27 G pencil-point tip. *Br J Anaesth*. 2012;108(2):308-315.
25. Asakura T, Seino H, Nunoi K, et al. Usability of a microtapered needle (TN3305) for insulin treatment in Japanese patients with diabetes mellitus: a comparative clinical study with a standard thin wall needle. *Diabetes Technol Ther*. 2006;8(4):489-494.
26. Allmendinger A, Fischer S, Huwyler J, et al. Rheological characterization and injection forces of concentrated protein formulations: an alternative predictive model for non-Newtonian solutions. *Eur J Pharm Biopharm*. 2014;87(2):318-328.
27. Rathore N, Pranay P, Bernacki J, Eu B, Ji W, Walls E. Characterization of protein rheology and delivery forces for combination products. *J Pharm Sci*. 2012;101(12):4472-4480.
28. Yoshino K, Nakamura K, Yamashita A, et al. Functional evaluation and characterization of a newly developed silicone oil-free prefillable syringe system. *J Pharm Sci*. 2014;103(5):1520-1528.
29. Kim H, Park H, Lee SJ. Effective method for drug injection into subcutaneous tissue. *Sci Rep*. 2017;7(1):9613.
30. Benchabane A, Bekkour K. Rheological properties of carboxymethyl cellulose (CMC) solutions. *Colloid Polym Sci*. 2008;286(10):1173-1180.
31. Bee JS, Stevenson JL, Mehta B, et al. Response of a concentrated monoclonal antibody formulation to high shear. *Biotechnol Bioeng*. 2009;103(5):936-943.
32. Piedmonte DM, Gu JH, Brych SR, Goss MM. Practical considerations for high concentration protein formulations. In: Warne NW, Mahler H-C, eds. *Challenges in Protein Product Development*. Cham: Springer International Publishing; 2018:163-187.
33. De Bardi M, Muller R, Grunzweig C, et al. Clogging in staked-in needle pre-filled syringes (SIN-PFS): influence of water vapor transmission through the needle shield. *Eur J Pharm Biopharm*. 2018;127:104-111.
34. Allmendinger A, Mueller R, Schwarb E, et al. Measuring tissue backpressure—in vivo injection forces during subcutaneous injection. *Pharm Res*. 2015;32(7):2229-2240.